Inorg. Chem. **2006**, *45*, 9959–9973

Forum

Assessing the Integrity of Designed Homomeric Parallel Three-Stranded Coiled Coils in the Presence of Metal Ions

Olga Iranzo,[†] Debdip Ghosh,[†] and Vincent L. Pecoraro*[,†,‡]

Department of Chemistry and Biophysics Research Division, University of Michigan, Ann Arbor, Michigan 48109-1055

Received June 28, 2006

De novo design of α-helical peptides that self-assemble to form helical coiled coils is a powerful tool for studying molecular recognition between peptides/proteins and determining the fundamental forces involved in their folding and structure. These amphipathic helices assemble in aqueous solution to generate the final coiled coil motif, with the hydrophobic residues in the interior and the polar/hydrophilic groups on the exterior. Considerable effort has been devoted to investigate the forces that determine the overall stability and final three-dimensional structure of the coiled coils. One of the major challenges in coiled coil design is the achievement of specificity in terms of the oligomeric state, with respect to number (two, three, four, or higher), nature (homomers vs heteromers), and strand orientation (parallel vs antiparallel). As seen in nature, metal ions play an important role in this self-organization process, and the overall structure of metalloproteins is primarily the result of two driving forces: the metal coordination preference and the fold of the polypeptide backbone. Previous work in our group has shown that metal ions such as As(III) and Hg(II) can be used to enforce different aggregation states in the Cys derivatives of the designed homotrimeric coiled-coil TRI family [Ac-G(LKALEEK)$_4$G-CONH$_2$]. We are now interested in studying the interplay between the metal ion and peptide preferences in controlling the specificity and relative orientation of the α-helices in coiled coils. For this objective, two derivatives of the TRI family, TRi L2WL9C and TRi L2WL23C, have been synthesized. Along with those two peptides, two derivatives of Coil-Ser, CSL9C and CSL19C (CS = Ac-EWEALEKKLAALESKLQALEKKLEALEHG-CONH$_2$), a similar *de novo* designed three-stranded coiled coil that has the potential to form antiparallel coiled coils, have also been used. Circular dichroism, UV–vis, and ^{199}Hg and ^{113}Cd NMR spectroscopy results reveal that the addition of Hg(II) and Cd(II) to the different mixtures of these peptides forms preferentially homotrimeric coiled coils, over a statistical population of heterotrimeric parallel and antiparallel coiled coils.

Introduction

De novo peptide design provides us with the opportunity to study protein interactions and folding using first principles.[1−3] The most commonly employed structural patterns include the α-helical coiled coils,[2,4,5] the $\beta_2\alpha$ motif for Zn-binding proteins,[6−8] and β-sheet like proteins.[9] The coiled coil motif is a relatively simple structure in which two or more amphipathic α-helices supercoil around each other with a slight left-handed twist. These α-helices contain a characteristic repeat of seven residues (**abcdefg**) called a heptad, with hydrophobic residues occupying the **a** and **d** positions

* To whom correspondence should be addressed. E-mail: vlpec@umich.edu.
† Department of Chemistry.
‡ Biophysics Research Division.

(1) DeGrado, W. F.; Summa, C. M.; Pavone, V.; Nastri, F.; Lombardi, A. *Annu. Rev. Biochem.* **1999**, *68*, 779−819.
(2) Lombardi, A.; Summa, C. M.; Geremia, S.; Randaccio, L.; Pavone, V.; DeGrado, W. F. *Proc. Natl. Acad. Sci. U.S.A.* **2000**, *97*, 6298−6305.
(3) Nastri, F.; Lombardi, A.; Pavone, V. *Chem. Rev.* **2001**, *101*, 3165−3189.
(4) Dieckmann, G. R.; McRorie, D. K.; Tierney, D. L.; Utschig, L. M.; Singer, C. P.; O'Halloran, T. V.; Penner-Hahn, J. E.; DeGrado, W. F.; Pecoraro, V. L. *J. Am. Chem. Soc.* **1997**, *119*, 6195−6196.
(5) Gibney, B. R.; Dutton, P. L. *Protein Sci.* **1999**, *8*, 1888−1898.
(6) Krizek, B. A.; Amann, B. T.; Kilfoil, V. J.; Merkle, D. L.; Berg, J. M. *J. Am. Chem. Soc.* **1991**, *113*, 4518−4523.
(7) Struthers, M. D.; Cheng, R. P.; Imperiali, B. *Science* **1996**, *271*, 342−345.

10.1021/ic061183e CCC: $33.50
Published on Web 12/04/2006

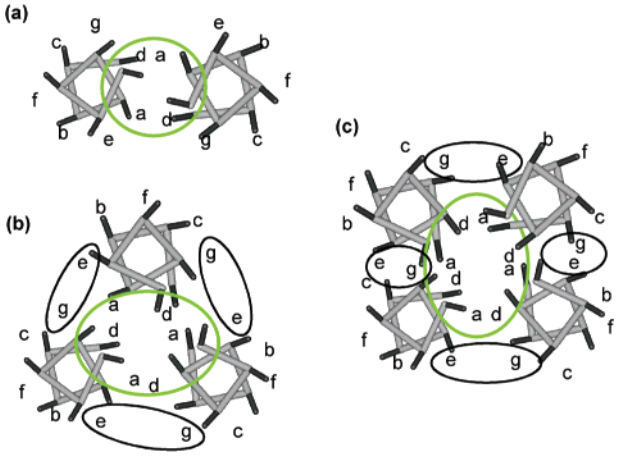

Figure 1. Helical wheel diagram showing the hydrophobic (green) and electrostatic (black) interactions for parallel two- (a), three- (b), and four-stranded (c) coiled-coil peptides. Reprinted from ref 10. Copyright 2004 American Chemical Society.

of this cassette and polar residues placed at the **e** and **g** positions. These amphipathic helices aggregate in aqueous solution to generate the final coiled coil motif, with the hydrophobic residues in the interior and the polar/hydrophilic groups on the exterior. As shown below, considerable effort has been devoted to understanding how these two main forces, hydrophobic packing and electrostatic interactions, can determine the overall stability and final three-dimensional structure of the coiled coils. A helical wheel diagram that illustrates these two types of interactions for parallel oriented coiled coils is given in Figure 1. One of the major challenges in coiled coil design is the achievement of specificity in terms of the oligomeric state, in both number (two, three, four, or higher) and nature (homomers vs heteromers), and strand orientation (parallel vs antiparallel). When metal binding sites are engineered in these *de novo* designed coiled coils and metal ions are present during the process of assembly, further factors come into play that can mediate and dictate the specific aggregation state, nature, and relative orientation of the α-helices. A previous *Inorganic Chemistry* Forum on Metalloprotein Folding provided Articles that address some of these issues with homomeric systems.[10,11] This Article will summarize work that was helpful to clarify the factors that determine the stability and final structure of *de novo* designed coiled coils with an emphasis in heteromeric systems.

Homomeric Coiled Coils. The vast majority of *de novo* designed coiled coils are formed by the assembly of separate α-helical chains in a homomeric association. This folding pattern occurs both in parallel[12−15] and in antiparallel orientations.[16−18] Hodges *et al*. demonstrated that electrostatic interactions between polar/charged residues at the **e** and **g** positions could play a major role in protein folding by controlling the parallel or antiparallel alignment of the α-helices in coiled coils.[19,20] Alternately, Hodges *et al*. also showed that when these types of interactions were not crucial in determining the orientation of the α-helices, the relative positions of Ala residues in the hydrophobic core of the middle heptad became the major factor controlling the parallel or antiparallel orientations of the chains in the final four-stranded coiled coil.[21] Highlighting the role of steric matching of hydrophobic side chains, the formation in the middle heptad of two layers of hydrophobic packing of the type Ala-Leu-Ala-Leu (antiparallel orientation) vs the formation of the layers Ala-Ala-Ala-Ala and Leu-Leu-Leu-Leu (parallel orientation) was the driving force in determining coiled coil topology. Consistent with these results, Oakley *et al*. designed a homodimeric antiparallel coiled coil using simultaneous application of electrostatic interactions and steric matching in the hydrophobic core by the introduction of Ala residues.[22] Recent studies by Lu *et al*. showed that the selection of polar/charged or nonpolar residues at the **g** position might provide an additional mechanism to control both the aggregation number and the helix orientation in coiled coils.[23] In a recent work, Ghadiri *et al*. demonstrated, using GCN4-derived peptides, how a single solvent-exposed amino substitution, in particular replacement of a Glu residue at the **f** position of the third heptad by Cys or Ser residues, can control the relative orientation of the helices in a homotetrameric coiled coil. In addition, they show how, depending on experimental conditions, the Ser-derivative peptide is able to crystallize in both conformations, parallel and antiparallel, suggesting that the energetic difference between these two assemblies is small enough to allow the switch (Figure 2).[24]

Heteromeric Coiled Coils. While substantial progress has been achieved toward understanding the main factors that specify and stabilize both parallel and antiparallel homomeric coiled coils, less is known regarding the formation of heteromeric coiled coils. In fact, there are few examples seen in *de novo* peptide chemistry where heteromeric coiled coils have been studied. An additional factor to consider in the design of heteromeric coiled coils is the fact that individual strands must assemble into a specific aggregation state to avoid the formation of a statistical combination of helices

(8) Struthers, M. D.; Cheng, R. P.; Imperiali, P. *J. Am. Chem. Soc.* **1996**, *118*, 3073−3081.
(9) Venkatraman, J.; Naganagowda, G. A.; Sudha, R.; Balaram, P. *Chem. Commun.* **2001**, 2660−2661.
(10) Ghosh, D.; Pecoraro, V. L. *Inorg. Chem.* **2004**, *43*, 7902−7915.
(11) Doerr, A. J.; McLendon, G. L. *Inorg. Chem* **2004**, *43*, 7916−7925.
(12) DeGrado, W. F.; Wasserman, Z. R.; Lear, J. D. *Science* **1989**, *243*, 622−628.
(13) Dieckmann, G. R.; McRorie, D. K.; Lear, J. D.; Sharp, K. A.; DeGrado, W. F.; Pecoraro, V. L. *J. Mol. Biol.* **1998**, *280*, 897−912.
(14) Ghadiri, M. R.; Choi, C. *J. Am. Chem. Soc.* **1990**, *112*, 1630−1632.
(15) Gibney, B. R.; Mulholland, S. E.; Rabanal, F.; Dutton, P. L. *Proc. Natl. Acad. Sci. U.S.A.* **1996**, *93*, 15041−15046.
(16) Betz, S. F.; DeGrado, W. F. *Biochemistry* **1996**, *35*, 6955−6962.
(17) Betz, S. F.; Liebman, A.; DeGrado, W. F. *Biochemistry* **1997**, *36*, 2450−2458.
(18) Ghirlanda, G.; Lear, J. D.; Ogihara, N.; Eisenberg, D.; DeGrado, W. F. *J. Mol. Biol.* **2002**, *319*, 243−253.
(19) Monera, O. D.; Zhou, N. E.; Kay, C. M.; Hodges, R. S. *J. Biol. Chem.* **1993**, *268*, 19218−19227.
(20) Monera, O. D.; Kay, C. M.; Hodges, R. S. *Biochemistry* **1994**, *33*, 3862−3871.
(21) Monera, O. D.; Zhou, N. E.; Lavigne, P.; Kay, C. M.; Hodges, R. S. *J. Biol. Chem.* **1996**, *271*, 3995−4001.
(22) Gurnon, D. G.; Whitaker, J. A.; Oakley, M. G. *J. Am. Chem. Soc.* **2003**, *125*, 7518−7519.
(23) Deng, Y.; Liu, J.; Zheng, Q.; Eliezer, D.; Kallenbach, N. R.; Lu, M. *Structure* **2006**, *14*, 247−255.
(24) Yadav, M. K.; Leman, L. J.; Price, D. J.; Brooks, C. L., III; Stout, C. D.; Ghadiri, M. R. *Biochemistry* **2006**, *45*, 4463−4473.

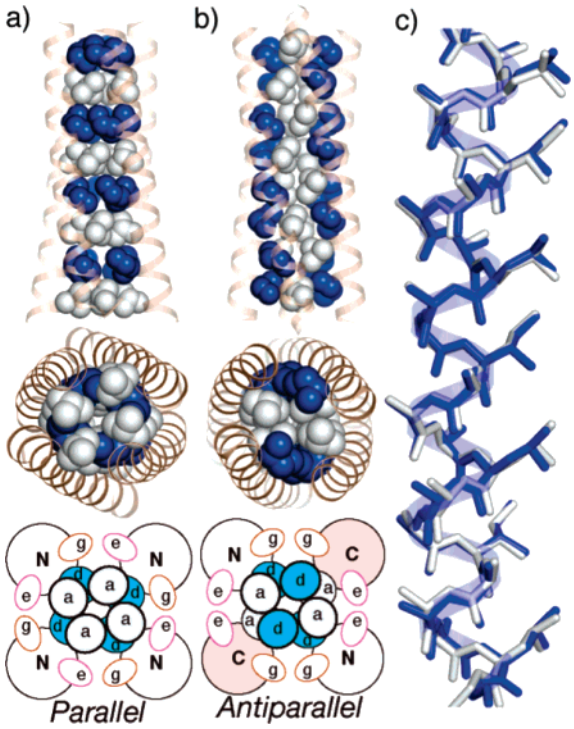

Figure 2. Crystal structures of the E20S variant in the tetrameric parallel and antiparallel configurations. Side and top views show the parallel (a) and antiparallel (b) structures, highlighting core Leu (white) and Ile (blue) residues, with schematic diagrams showing interhelical packing interactions. (c) Superposition of single helices from the antiparallel (blue) and parallel (beige) configurations. Backbone, α carbons, and core residue heavy atoms are shown (see ref 24). Copyright 2006 American Chemical Society.

including the formation of homomeric coiled coils. On the basis of the Fos/Jun Leu−zipper heterodimer system, where the destabilization of the Fos homodimer is the driving force for the preferential pairing of the Fos and Jun peptides, Kim *et al*. successfully designed the peptide "Velcro", a heterodimeric coiled coil (Acid-p1-Base-p1).[25] The peptides, Acid-p1 and Base-p1, were designed to contain only Glu and Lys residues at both the **e** and **g** positions, respectively, and a single Asn residue at position **a** in the second heptad (position 14) to favor the parallel orientation of the helices. This strategy favored mainly the formation of the parallel heterodimer by the electrostatic destabilization of the homodimers. Later on, they showed that whereas replacement of the buried Asn14 residue with Leu in the heterodimeric "Velcro" coiled coil significantly increased the association affinity of the complex, the mutation led to a preferential formation of a heterotetramer lacking a unique arrangement of helices. These results point out that a single buried polar interaction in the hydrophobic core of coiled coils is capable of imparting specificity in the final structures at the expense of stability.[26] In a later report, Kim *et al*. showed that, instead of replacement, alteration in the position of the buried Asn14 residue led to a change in the relative orientation of the helices, resulting in the formation of a more stable and preferred (2.3 kcal/mol) heterodimeric antiparallel coiled coil

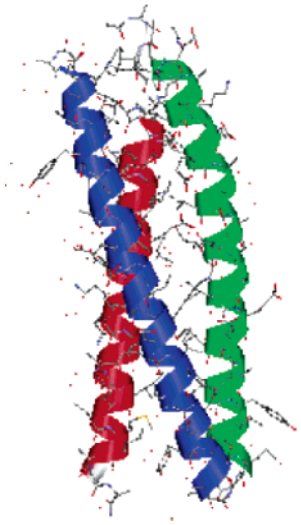

Figure 3. Crystal structure of the designed thermostable heterotrimeric coiled-coil peptide ABC (PDB code 1BB1; see ref 31).

(Acid-a1-Base-a1).[27] Oakley *et al*. further demonstrated that replacement of a single residue at a **g** position in each of the peptides, Acid-a1 and Base-a1, resulted in the exclusive formation of the heterodimeric antiparallel coiled coil.[28,29]

Using a similar strategy of negative design in which attractive electrostatic interactions between **g** and **e** residues were maximized in the heterotrimer aggregate and repulsive interactions were maximized in the alternative species, Alber *et al*. demonstrated how peptides that have strong association affinities for each other could associate together to form selectively an ABC-type heterotrimeric coiled coil.[30] In separate work, this group explored in more detail the origin of this heterotrimer specificity and concluded that favorable electrostatic interactions were a determining factor in the stability of this polypeptide. Elucidation of a 1.8-Å resolution crystal structure (Figure 3) of this heteromeric peptide substantiated their hypothesis.[31] In a progressive study, Schnarr and Kennan have shown that specific ABC-type heterotrimers can be obtained from independent peptide strands by steric matching of multiple hydrophobic core side chains of Ala and cyclohexylalanines and hydrophilic matching of Glu and Lys residues at the **e** and **g** positions.[32,33] Later on, using the same principles, they designed an antiparallel ABC-type heterotrimer.[34] Recently, they have reported an antiparallel heterotrimer, with a single **e**/**g** mismatched electrostatic interface, that is able to switch to a parallel homotrimer using a pH-triggered strand exchange.[35] In a similar work, Tanaka *et al*. demonstrated the formation

(25) O'Shea, E. K.; Lumb, K. J.; Kim, P. S. *Curr. Biol.* **1993**, *3*, 658−667.
(26) Lumb, K. J.; Kim, P. S. *Biochemistry* **1995**, *34*, 8642−8648.
(27) Oakley, M. G.; Kim, P. S. *Biochemistry* **1998**, *37*, 12603−12610.
(28) McClain, D. L.; Binfet, J. P.; Oakley, M. G. *J. Mol. Biol.* **2001**, *313*, 371−383.
(29) McClain, D. L.; Woods, H. L.; Oakley, M. G. *J. Am. Chem. Soc.* **2001**, *123*, 3151−3152.
(30) Nautiyal, S.; Woolfson, D. N.; King, D. S.; Alber, T. *Biochemistry* **1995**, *34*, 11645−11651.
(31) Nautiyal, S.; Tom, A. *Protein Sci.* **1999**, *8*, 84−90.
(32) Schnarr, N. A.; Kennan, A. J. *J. Am. Chem. Soc.* **2002**, *124*, 9779−9783.
(33) Schnarr, N. A.; Kennan, A. J. *J. Am. Chem. Soc.* **2003**, 667−671.
(34) Schnarr, N. A.; Kennan, A. J. *J. Am. Chem. Soc.* **2004**, *126*, 14447−14451.
(35) Schnarr, N. A.; Kennan, A. J. *Org. Lett.* **2005**, *7*, 395−398.

of an A_2B heterotrimer using a pair of 31-residue peptides where replacement of the Ile at the **a** position in the second heptad of the parent peptide with Ala (IZ-2aA) or Trp (IZ-2aW) gave rise to peptides that weakly self-associate but, when mixed, afforded a stable $(IZ\text{-}2aA)_2$−IZ-2aW coiled coil.[36] Using the same principle, involving smaller Ala and bulky Trp residues, Tanaka *et al*. formed an ABC-type heterotrimer by replacement of the central three **a** positions of the three heptads with either Trp-Ala-Ala, Ala-Trp-Ala, or Ala-Ala-Trp assignments. In a separate report, the group further demonstrated that mutation of the Lys residues at the **f** positions to either an Ala or Gln residue (in addition to one or two Ala-Ala-Trp interactions in the hydrophobic core) resulted in selective formation of AAB- or ABC-type heterotrimers, respectively.[37] Novotny *et al*. designed an A_2B_2-type heterotetrameric coiled coil using Lac repressor-based peptides containing either Glu or Lys at all **b** and **c** positions. Their results show that incorporation of these charged residues at these positions gives rise to stabilizing Glu−Lys interactions that favor the formation of the heterotetramer over the homotetramer.[38]

These studies show that the introduction of either small non-polar residues, such as Ala, or larger residues, such as Trp or cyclohexylalanines, at **a** or **d** positions destabilizes the formation of homomeric coiled coils mainly because of either the steric void or steric hindrance that is generated in the hydrophobic core in the respective cases. However, the proper alignment of these residues to achieve sterically matched hydrophobic cores compensates for these disadvantages and dictates the formation of heteromeric coiled coils. Nonetheless, this steric matching is not always sufficient for specificity, and additional specificity can be achieved by fine-tuning the electrostatic matching or mismatching between the charged/polar residues located at the interfaces of the α-helices that form the coiled coil.

Heteromeric Metallopeptides. Contrary to the research carried out on heteromeric apopeptides, very little work has been pursued in designed heteromeric metallopeptides where side chains capable of binding metal ions have to be incorporated in the hydrophobic core of these coiled coils.[39−42] This type of design can generate metal binding sites that are made of different ligand donors, a limitation that homomeric systems have. On the basis of the sequence of the Coil-Ser (CS) peptide, DeGrado *et al*. designed three peptides, two containing His in the **a** position of the fourth heptad and one containing a Cys in the **d** position of the first heptad. When mixed, these peptides formed preferentially an ABC-type heterotrimer mainly because of favorable electrostatic interactions between the helices. The authors claimed an antiparallel arrangement of the helices and therefore the formation of a two-His, one-Cys trigonal metal binding site. However, they were unable to observe binding of Cu(II) and Co(II).[39] Later on, they designed a heterotetrameric antiparallel coiled coil of the type A_2B_2 capable of binding 2 equiv of Zn(II), Co(II), and Fe(II).[40] This coiled coil was computationally designed from the DF1 system by using a negative design and "minimalist" approaches. Peptide A contained Glu at the **a** position of the third heptad, and peptide B contained the E(**a**)XXH(**d**) metal binding motif in the heptad. Solution characterization of the system and metal binding suggested that the intended topology and metal binding pocket were achieved. Afterward, they modified the sequence of the A peptide to generate two different ones, one with Glu in the interface (A_a) and the other with Lys and Arg at the equivalent positions (A_b). This design gave rise to an $A_aA_bB_2$ heterotetrameric coiled coil that also interacted with Zn(II), Co(II), and Fe(II).[41] On the basis of their previous heteromeric coiled coil designs, Tanaka *et al*. demonstrated that placement of two His residues at the **a** and **d** positions of the third heptad and either an Ala or Trp residue at the **a** position of the first heptad resulted in the formation of a metal [Ni(II)]-induced A_2B-type heterotrimer.[42] In the absence of metal, neither the peptides nor the peptide mixtures self-associated to form stable coiled coils.

TRI Family of Coiled Coils. All of the peptidic coiled coils of the TRI family of peptides (TRI LXC) that have been investigated so far in our group form parallel three-stranded coiled coils above pH 6, showing that the intended initial design was always achieved.[4,43−45] This approach generated a Cys-rich metal binding site capable of binding metals such as Hg(II),[4] Cd(II),[44] Pb(II),[46] Bi(III),[46] and As(III).[47] However, a significant outstanding question with this system is, how would mixtures of peptides behave, especially in the presence of metals that might stabilize less common peptide aggregates due to the strong metal−S bonds? Thus, if one were to prepare mixtures of the TRI L9C and TRI L23C peptides that could in theory bind metals as homomeric parallel coiled coils or heterotrimeric antiparallel coiled coils, would one form exclusively metalated peptides that corresponded to the desired $M(TRI\ L9C)_3$ and $M(TRI\ L23C)_3$ assemblies or would one lose all specificity and generate statistical mixtures of $M(TRI\ L9C)_{3-n}(TRI\ L23C)_n$ (where $n = 0-3$)? This has been a classic question in small molecule recognition chemistry; however, this important concept has not been addressed in designed peptide

(36) Kashiwada, A.; Hiroaki, H.; Kohda, D.; Nango, M.; Tanaka, T. *J. Am. Chem. Soc.* **2000**, *122*, 212−215.
(37) Kiyokawa, T.; Kanaori, K.; Tajima, K.; Mizuno, T.; Oku, J.; Tanaka, T. *Chem.—Eur. J.* **2004**, *10*, 3548−3554.
(38) Fairman, R.; Chao, H.-G.; Lavoie, T. B.; Villafranca, J. J.; Matsueda, G. R.; Novotny, J. *Biochemistry* **1996**, *35*, 2824−2829.
(39) Lombardi, A.; Bryson, J. W.; DeGrado, W. F. *Biopolymers* **1997**, *40*, 495−504.
(40) Summa, C. M.; Rosenblatt, M. M.; Hong, J.-K.; Lear, J. D.; DeGrado, W. F. *J. Mol. Biol.* **2002**, *321*, 923−938.
(41) Marsh, E. N. G.; DeGrado, W. F. *Proc. Natl. Acad. Sci. U.S.A.* **2002**, *99*, 5150−5154.
(42) Kiyokawa, T.; Kanaori, K.; Tajima, K.; Tanaka, T. *Biopolymers* **2000**, *55*, 407−414.
(43) Farrer, B. T.; Harris, N. P.; Balchus, K. E.; Pecoraro, V. L. *Biochemistry* **2001**, *40*, 14696−14705.
(44) Matzapetakis, M.; Farrer, B. T.; Weng, T.-C.; Hemmingsen, L.; Penner-Hahn, J. E.; Pecoraro, V. L. *J. Am. Chem. Soc.* **2002**, *124*, 8042−8054.
(45) Ghosh, D.; Lee, K.-H.; Demeler, B.; Pecoraro, V. L. *Biochemistry* **2005**, *44*, 10732−10740.
(46) Matzapetakis, M.; Ghosh, D.; Weng, T.-C.; Penner-Hahn, J. E.; Pecoraro, V. L. *J. Biol. Inorg. Chem.* **2006**, *11*, 876−890.
(47) Farrer, B.; McClure, C.; Penner-Hahn, J. E.; Pecoraro, V. L. *Inorg. Chem.* **2000**, *39*, 5422−5423.

Figure 4. Crystal structure of the designed antiparallel three-stranded coiled-coil peptide Coil-Ser (PDB code 1COS). The side chain of the Trp residues is shown in blue (see ref 48).

systems. The answer to these questions will allow us to assess the strength of our original homomeric designs.

It should be noted that our concern with the lack of design specificity already has some precedent in related three-stranded coiled coils. The classic example of a *de novo* designed homomeric antiparallel peptide is Coil-Ser, prepared by DeGrado *et al*.[48] Coil-Ser was crystallographically characterized at pH 5 and, surprisingly, formed an antiparallel three-stranded coiled coil, although studies at higher pH suggested that parallel structures dominated. This peptide has design similarities with the TRI peptides but differs in key aspects in the primary sequence; most notably, Coil-Ser has a Trp residue at the second position of the sequence. One of the hypotheses for the antiparallel nature of the aggregate was the presence of these large Trp residues. It was felt that the presence of three large residues at the same level was sterically unfavorable, consequently leading to flipping of one of the strands and thereby generating Trp-Trp-Leu and Trp-Leu-Leu layers (Figure 4). This residue arrangement would be less sterically demanding and, thus, would consequently lead to the antiparallel orientation of the peptide. Consistent with this observation, a parallel trimer, Coil-V_aL_d, was obtained when the residues at the **a** positions in Coil-Ser were replaced by Val.[49] Along these lines, the recent work by Ghadiri *et al*., previously described, represents another example of structural nonspecificity in coiled coil peptides because a single peptide sequence is able to generate homotetrameric coiled coils that crystallize in both parallel and antiparallel configurations.[24]

Taking into account these results, we were interested in *knowing* if our original design could stand the test of generating precisely defined and predicted homomeric assemblies under conditions where mixtures might easily be obtained. If we were successful in retaining molecular specificity, we then wished to address whether sequence modifications could easily perturb the species distribution in these peptides. The simple replacement of the Leu residue at the second position of the TRI LXC family with a Trp residue would be the most conservative change to test the ability to generate antiparallel three-stranded TRI peptides. Two derivatives of TRI with a Trp residue at the second position and a Cys either at the 9th position (TRI L2WL9C) or at the 23rd position (TRI L2WL23C) were synthesized (see Table 1 for sequences). The rationale behind this design was that the flipping of a strand of the TRI L2WL9C peptide would position the Cys residue at or near the 23rd Cys residue of the TRI L2WL23C. Thus, if heterotrimeric antiparallel coiled coils could be generated with two strands of TRI L2WL9C and one of TRI L2WL23C or vice versa, they would generate a Cys-rich binding site that was essentially equivalent to the homomeric assembly because the thiol groups would be at about the same level. Along with the study involving TRI peptides, a parallel analysis was carried out with derivatives of the parent Coil-Ser peptide. Two peptides, Coil-Ser L9C (CSL9C) and Coil-Ser L19C (CSL19C), were synthesized using this rationale (see Table 1 for sequences). Binding of Hg(II) and Cd(II) to both the Trp derivatives of TRI LXC and the CSLXC families was studied by different spectroscopic techniques to interrogate the nature of these systems.

Results

Binding of Hg(II) and Cd(II) to Homotrimers. (a) UV−Vis Spectroscopy. The formation of the Hg(II) and Cd(II) complexes with the Trp derivatives of TRI L9C and TRI L23C and with CSL9C and CSL19C was monitored by UV−vis spectroscopy using the ligand-to-metal charge-transfer (LMCT) bands at 235 and 247 nm for Cd−S or Hg−S bonds, respectively, as was done previously for the TRI family.[4,44]

(i) Binding of Hg(II) and Cd(II) to TRI Peptides. The addition of 2 equiv of TRI L2WL9C to a solution of $HgCl_2$ generates the signature charge-transfer band at 240 nm for linear HgS_2.[4] The addition of 1 equiv more of TRI L2WL9C to the moiety Hg(TRI L2WL9C)$_2$ generates the trigonal Hg(II) complex as seen by the growth of the charger-transfer band at 247 nm (Figure S1a in the Supporting Information). A similar spectrum is observed upon the addition of TRI L2WL23C into $HgCl_2$. The stability constants (K_{bind}) for binding of the third thiolate to linear Hg(TRI L2WL9C)$_2$

Table 1. List of Peptides Used in This Research with Their Sequences

peptide	sequence
TRI L9C	Ac-G LKALEEK **C**KALEEK LKALEEK LKALEEK G-NH_2
TRI L23C	Ac-G LKALEEK LKALEEK LKALEEK **C**KALEEK G-NH_2
TRI L2WL9C	Ac-G **W**KALEEK **C**KALEEK LKALEEK LKALEEK G-NH_2
TRI L2WL23C	'Ac-G **W**KALEEK LKALEEK LKALEEK **C**KALEEK G-NH_2
CSL9C	Ac-E WEALEKK **C**AALESK LQALEKK LEALEHG-NH_2
CSL19C	Ac-E WEALEKK LAALESK LQA**C**EKK LEALEHG-NH_2

Table 2. Comparison of Physical Parameters for Complexes of Cd(II) and Hg(II) with Derivatives of the Peptides TRI and Coil-Ser

complex	UV−vis: λ, nm ($\Delta\epsilon$ (M^{-1} cm^{-1}))	chemical shift (ppm) ^{199}Hg NMR	chemical shift (ppm) ^{113}Cd NMR	apparent pK_a	stability constant (M^{-1})
$Hg(TRI\ L9C)_3^-$	247 (20 200)	−185		7.6 ± 0.2[a]	3.6×10^7 [c]
$Hg(TRI\ L23C)_3^-$	247 (19 200)			7.6 ± 0.2	1.8×10^7
$Hg(TRI\ L2WL9C)_3^-$	247 (19 000)			7.6 ± 0.2	4.7×10^6
$Hg(TRI\ L2WL23C)_3^-$	247 (18 900)				
$Hg(CSL9C)_3^-$	247 (15 550)	−185		7.3 ± 0.2	2.0×10^7 [e]
$Hg(CSL19C)_3^-$	229 (17 000)	−313		8.6 ± 0.2	2.3×10^6
$Cd(TRI\ L9C)_3^-$	233 (22 300)		615	13.4 ± 0.2[b]	1.2×10^8 [d]
$Cd(TRI\ L23C)_3^-$	233 (22 300)		612	13.4 ± 0.2	8.8×10^7
$Cd(TRI\ L2WL9C)_3^-$	233 (22 200)		618	13.4 ± 0.2	8.8×10^7
$Cd(TRI\ L2WL23C)_3^-$			611		
$Cd(CSL9C)_3^-$	235 (19 000)		602	13.2 ± 0.2	2.7×10^7 [e]
$Cd(CSL19C)_3^-$	235 (21 000)		628	14.6 ± 0.2	1.7×10^7

[a] The model used to obtain the pK_a for Hg(II) peptides is $Hg^{II}(RS)_2(H-RS) \leftrightarrows Hg^{II}(RS)_3^- + H^+$ (K_a). [b] The model used to obtain the pK_a for Cd(II) peptides is $M^{II}(RS)(H-RS)_2^+ \leftrightarrows M^{II}(RS)_3^- + 2H^+$ (K_{a2}). [c] The model used to obtain stability constants for Hg(II) binding is $Hg(RS)_2 + RS^- \leftrightarrows Hg^{II}(RS)_3^-$ (K_b). [d] The model used to obtain stability constants for Cd(II) binding is $M^{II} + (RS)_3^{3-} \leftrightarrows M^{II}(RS)_3^-$ (K_b). [e] These values represent the lower limit value for the obtained stability constants.

and $Hg(TRI\ L2WL23C)_2$ to form the corresponding trigonal complexes were calculated using the models explained in the Supporting Information and values are reported in Table 2.

The addition of 3 equiv of TRI L2WL9C into a solution of $CdCl_2$ generates the formation of the trigonal thiolate Cd(II) complex, $Cd(TRI\ L2WL9C)_3^-$, observed from the very beginning of the titration, as shown by the growth of the characteristic LMCT band at 235 nm (Figure S1b in the Supporting Information). The stability constant (K_{bind}) for binding of Cd(II) to this peptide was calculated using the model explained in the Supporting Information and the value is reported in Table 2.

(ii) Binding of Hg(II) and Cd(II) to Coil-Ser Peptides. A pattern similar to that observed for the binding of Hg(II) to the TRI family was observed for the titration of CSL9C into a solution of Hg(II) at pH 8.5, as shown in Figure 5a. The addition of 2 equiv of CSL9C to a solution of Hg(II) at pH 8.5 generates the linear complex $Hg(CSL9C)_2$. When the third equiv of CSL9C is added, the characteristic LMCT excitation at 247 nm corresponding to the formation of the trigonal complex $Hg(CSL9C)_3^-$ is observed. A similar spectrum was obtained for the titration of CSL19C into a solution of Hg(II) at pH 9.5. The stability constants (K_{bind}) for binding of the third thiolate to linear $Hg(CSL9C)_2$ and $Hg(CSL19C)_2$ to form the corresponding trigonal complexes $Hg(CSL9C)_3^-$ and $Hg(CSL19C)_3^-$ were calculated using the model explained in the Supporting Information, and values are reported in Table 2. Because these stability constants are relatively similar in magnitude and are only directly relevant at high pH, a better reflection of the formation of the complexes $Hg(CSL9C)_3^-$ and $Hg(CSL19C)_3^-$ in the neutral to weakly basic pH range is given by the pK_a values shown in Table 2. The pH dependence of the formation of the complexes $Hg(CSL9C)_3^-$ and $Hg(CSL19C)_3^-$ was monitored at 247 nm, and the pH titration curves are shown in Figure 6a. The formation of the trigonal thiolate Hg(II) complexes occurs at a significantly lower pH value for CSL9C (**a** site) than CSL19C (**d** site). The experimental data are consistent with the release of a single proton, and they

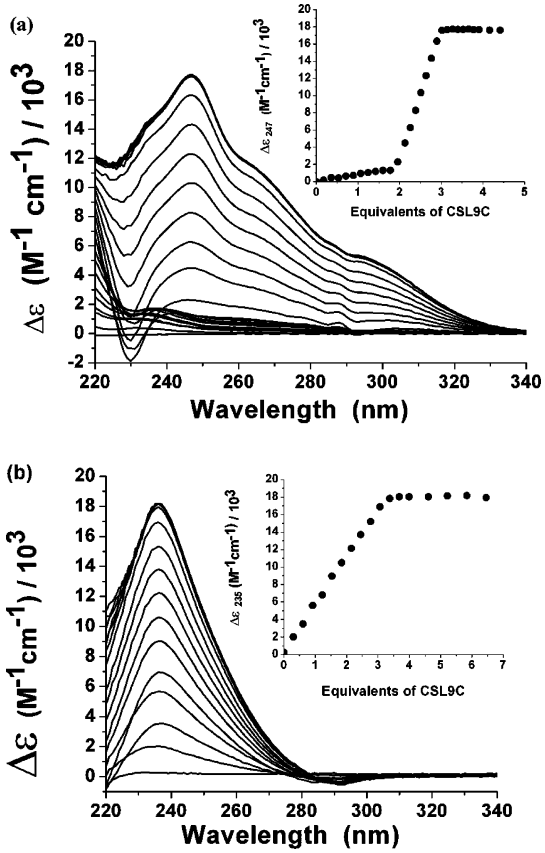

Figure 5. (a) Difference titration of CSL9C into a solution of Hg(II) (10 μM) at pH 8.5 (50 mM phosphate buffer). The inset of the figure shows the titration curve obtained by plotting the change in the absorbance at 247 nm as a function of the equivalents of peptide added. (b) Difference titration of CSL9C into a solution of Cd(II) (10 μM) at pH 8.5 (50 mM TRIS buffer). The inset of the figure shows the titration curve obtained by plotting the change in the absorbance at 235 nm as a function of the equivalents of peptide added.

(48) Lovejoy, B.; Choe, S.; Cascio, D.; McRorie, D. K.; DeGrado, W. F.; Eisenberg, D. *Science* **1993**, *259*, 1288−1293.
(49) Ogihara, N. L.; Weiss, M. S.; DeGrado, W. F.; Eisenberg, D. *Protein Sci.* **1997**, *6*, 80−88.

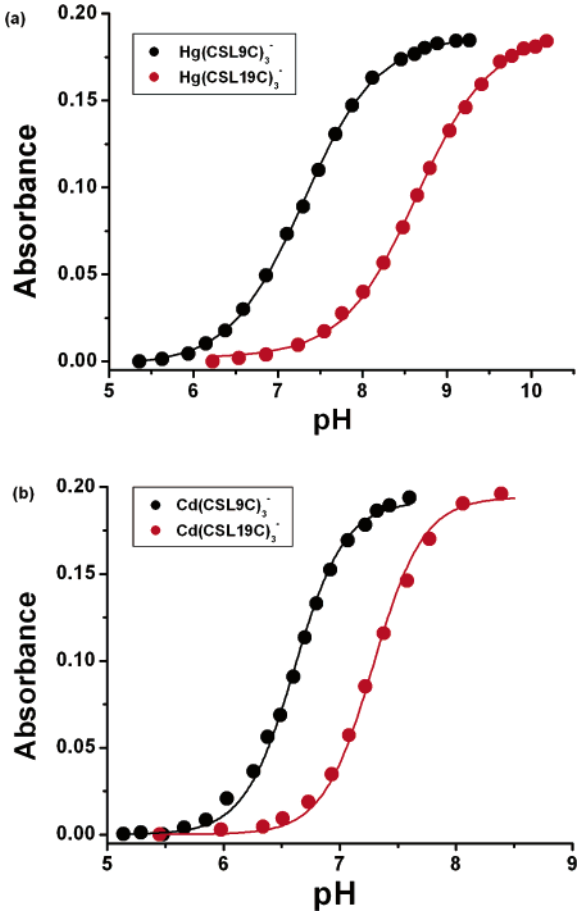

Figure 6. pH dependence of complex formation for (a) $Hg(CSL9C)_3^-$ (10 μM) and $Hg(CSL19C)_3^-$ (10 μM) and (b) $Cd(CSL9C)_3^-$ (10 μM) and $Cd(CSL19C)_3^-$ (10 μM). The lines represent the fits to the models explained in the Results section.

were fit using the model explained in the Supporting Information. pK_a values of 7.3 and 8.6 were obtained for the formation of $Hg(CSL9C)_3^-$ and $Hg(CSL19C)_3^-$, respectively.

Figure 5b shows the UV−vis spectra obtained for the titration of CSL9C into a solution of Cd(II) at pH 8.5. Formation of the trigonal thiolate Cd(II) complex $Cd(CSL9C)_3^-$ is observed from the very beginning, as the growth of the characteristic LMCT at 235 nm shows. Binding of Cd(II) to CSL19C at pH 8.5 followed the same pattern. The stability constants (K_{bind}) for binding of Cd(II) to these peptides were calculated using the model explained in the Supporting Information, and values are reported in Table 2. As mentioned above for the Hg(II) complexes, these stability constants are relatively close in magnitude; therefore, a better reflection of the formation of the complexes $Cd(CSL9C)_3^-$ and $Cd(CSL19C)_3^-$ at neutral to slightly basic conditions is given by the pK_a values shown below. The pH dependence of the formation of the complexes $Cd(CSL9C)_3^-$ and $Cd(CSL19C)_3^-$ was monitored at 235 nm, and the pH titration curves are shown in Figure 6b. As was observed for Hg(II), the formation of the trigonal thiolate Cd(II) complexes occurs at a lower pH value for CSL9C (**a** site) than CSL19C (**d** site). The shape of the pH titration curves is consistent with the release of two protons and, therefore,

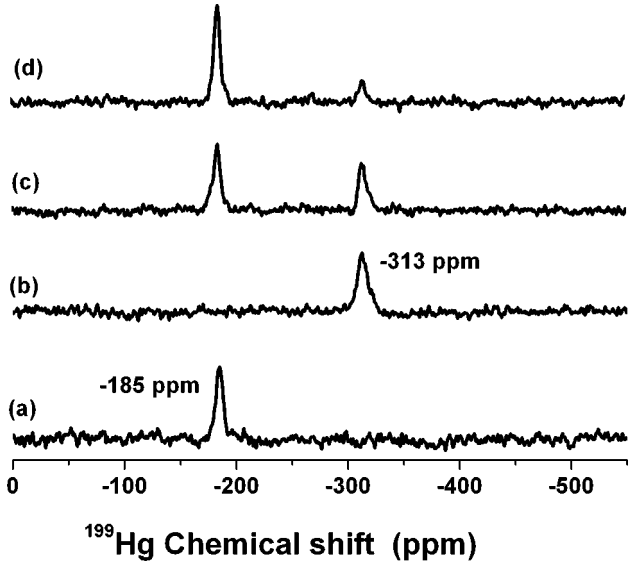

Figure 7. ^{199}Hg NMR spectra of solutions containing 3 mM $^{199}Hg(NO_3)_2$ and different ratios of CSL9C and CSL19C peptides: (a) 3 equiv of CSL9C at pH 8.5 (the same spectrum was obtained at pH 9.6); (b) 3 equiv of CSL19C at pH 9.6; (c) 2 equiv of CSL9C and 1 equiv of CSL19C at pH 9.6; (d) 1 equiv of CSL9C and 2 equiv of CSL19C at pH 9.6.

the best fit to the experimental data was obtained using model b and eq 5 (see the Supporting Information), which describes a two-proton dissociation step (K_{a2}) from the moiety Cd(RS)-$(RSH)_2^+$ to form $Cd(RS)_3^-$. pK_{a2} values of 13.2 and 14.6 were obtained for the formation of $Cd(CSL9C)_3^-$ and $Cd(CSL19C)_3^-$, respectively. This pH profile was also observed for binding of Cd(II) to the TRI family and implicates the formation of a $Cd(RS)(RSH)_2^+$ species at low pH, which does not contribute to the observed UV−vis spectroscopic signature.[46] This lower effective pK_a is the result of Cd(II) binding to the thiol group, which lowers the corresponding pK_a of the free thiol.

(b) Circular Dichroism (CD) Spectroscopy. We have shown that it is possible to observe LMCT bands in the TRI system using CD spectroscopy even though the first coordination sphere of the metal is not chiral.[44] Consistent with this observation, the difference CD spectra of the Hg(II) and Cd(II) complexes of CSL9C and CSL19C at pH values corresponding to the complete formation of the metal complexes show electronic transitions that indicate the formation of the respective trigonal thiolate metal complexes (see Figure S2 in the Supporting Information). A comparison of the LMCT bands observed in the CD spectra of $Hg(CSL9C)_3^-$ with those of $Hg(CSL19C)_3^-$ reveals the opposite polarity of these electronic transitions in both complexes. A similar pattern was observed for the complexes $Cd(CSL9C)_3^-$ and $Cd(CSL19C)_3^-$ (see Figure S3 in the Supporting Information). These results are in agreement with those obtained for the TRI family and highlight the different environments that surround the metal ions in the **a** site (CSL9C) relative to the **d** site (CSL19C).[44]

(c) NMR Spectroscopy. ^{199}Hg and ^{113}Cd NMR spectroscopies are well-established methods to elucidate the coordination environment of Hg(II)[50−53] and Cd(II)[54−56] in complexes because their chemical shifts are very sensitive

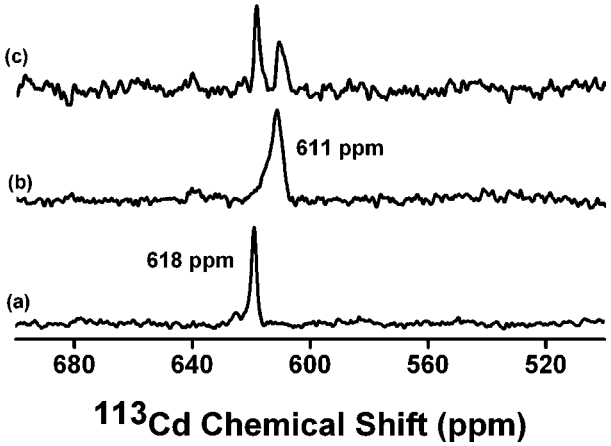

Figure 8. ^{113}Cd NMR spectra of solutions containing 3 mM $^{113}Cd(NO_3)_2$ and different ratios of TRI L2WL9C and TRI L2WL23C peptides at pH 8.5: (a) 3 equiv of TRI L2WL9C; (b) 3 equiv of TRI L2WL23C; (c) 2 equiv of TRI L2WL9C and 1 equiv of TRI L2WL23C.

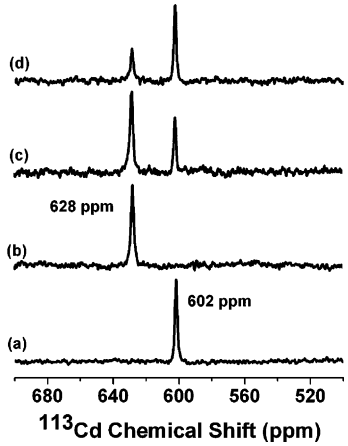

Figure 9. ^{113}Cd NMR spectra of solutions containing 3 mM $^{113}Cd(NO_3)_2$ and different ratios of CSL9C and CSL19C peptides at pH 8.5: (a) 3 equiv of CSL9C; (b) 3 equiv of CSL19C; (c) 2 equiv of CSL9C and 1 equiv of CSL19C; (d) 1 equiv of CSL9C and 2 equiv of CSL19C.

to the coordination number and ligand identity. The ^{199}Hg NMR spectra for the complexes $Hg(CSL9C)_3^-$ (pH 8.5) and $Hg(CSL19C)_3^-$ (pH 9.6) are shown in parts a and b of Figure 7, respectively. A single resonance is observed for both solutions with chemical shifts of −185 ppm for $Hg(CSL9C)_3^-$ and −313 ppm for $Hg(CSL19C)_3^-$. These data are consistent with thiol ligation to Hg(II) and, based on the results obtained for the TRI family, indicate a three-S environment.[4] The different ^{199}Hg NMR chemical shift observed infers a different environment in the **a** site compared to the **d** site. No other resonances were observed up to −1200 ppm, which suggests that the trigonal thiolate Hg(II) complexes were the only species in solution.

The ^{113}Cd NMR spectra for the complexes Cd(TRI L2WL9C)$_3^-$ and Cd(TRI L2WL23C)$_3^-$ at pH 8.5 are shown in parts a and b of Figure 8, respectively. A single resonance is observed for both solutions with chemical shifts of 618 ppm for Cd(TRI L2WL9C)$_3^-$ and 611 ppm for Cd(TRI L2WL23C)$_3^-$. Taking into account our previous studies of Cd(II) coordination in the TRI family,[57,58] these chemical shifts are indicative of a mixture of CdS_3^- and $CdS_3(O/N)$ coordination geometry, with the fourth ligand being most likely an exogenous water molecule. The ^{113}Cd NMR spectra for the complexes Cd(CSL9C)$_3^-$ and Cd(CSL19C)$_3^-$ at pH 8.5 are shown in parts a and b of Figure 9, respectively. A single resonance is similarly observed for both solutions with chemical shifts of 602 ppm for Cd(CSL9C)$_3^-$ and 628 ppm for Cd(CSL19C)$_3^-$. Assuming that CSLXC peptides behave similarly to the TRI LXC peptides, these results also show the formation of a mixture of CdS_3^- and $CdS_3(O/N)$ species. Both ^{199}Hg and ^{113}Cd NMR spectroscopies show that the environments that surround Hg(II) and Cd(II) in an **a** site (CSL9C) and a **d** site (CSL19C) are different. These results corroborate those obtained by UV−vis and CD spectroscopies.

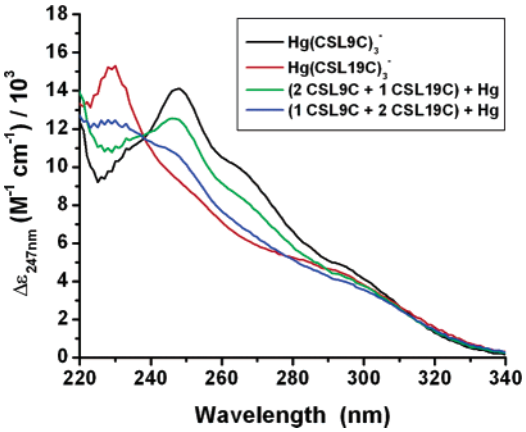

Figure 10. Difference UV−vis spectra of solutions containing 10 μM Hg(II) and different ratios of the peptides CSL9C and CSL19C at pH 9.5 (50 mM CHES buffer).

Binding of Hg(II) and Cd(II) to Mixtures of Peptides. (a) UV−Vis Spectroscopy. (i) Binding of Hg(II) to TRI Peptides. The addition of 2 equiv of TRI L2WL9C to a solution of Hg(II) at pH 8.5 generates the linear complex Hg(TRI L2WL9C)$_2$. The addition of the third equiv of peptide, in this case TRI L2WL23C, to this linear moiety generates the characteristic LMCT band at 247 nm, indicative of the formation of trigonal thiolate Hg(II) complexes. The final spectrum obtained for the mixture is very similar to that observed for the formation of the complexes Hg(TRI L2WL9C)$_3^-$ and Hg(TRI L2WL23C)$_3^-$.

(ii) Binding of Hg(II) to Coil-Ser Peptides. Shown in Figure 10 are the UV−vis spectra of solutions containing 10 μM Hg(II) and different equivalents of the peptides

(50) Wright, J. G.; Natan, M. J.; MacDonnell, F. M.; Ralston, D. M.; O'Halloran, T. V. *Prog. Inorg. Chem.* **1990**, *38*, 323−412.
(51) Wrackmeyer, B.; Contreras, R. *Annu. Rep. NMR. Spectrosc.* **1992**, *124*, 267−329.
(52) Utschig, L. M.; Wright, J. G.; Dieckmann, G. R.; Pecoraro, V. L.; O'Halloran, T. V. *Inorg. Chem.* **1995**, *34*, 2497−2498.
(53) Utschig, L. M.; Wright, J. G.; O'Halloran, T. V. *Methods Enzymol.* **1993**, *226*, 71−97.
(54) Corwin, D. T.; Gruff, E. S.; Koch, S. A. *J. Chem. Soc., Chem. Commun.* **1987**, 966−967.
(55) Corwin, D. T.; Gruff, E. S.; Koch, S. A. *Inorg. Chim. Acta* **1988**, *151*, 5−6.
(56) Gulin, O.; Poutney, D. L.; Armitage, I. M. *Biochem. Cell Biol.* **1998**, *76*, 223−243.
(57) Lee, K. H.; Matzapetakis, M.; Mitra, S.; Marsh, E. N. G.; Pecoraro, V. L. *J. Am. Chem. Soc.* **2004**, *126*, 9178−9179.
(58) Lee, K.-H.; Cabello, C.; Hemmingsen, L.; Marsh, E. N. G.; Pecoraro, V. L. *Angew. Chem., Int. Ed.* **2006**, *45*, 2864−2868.

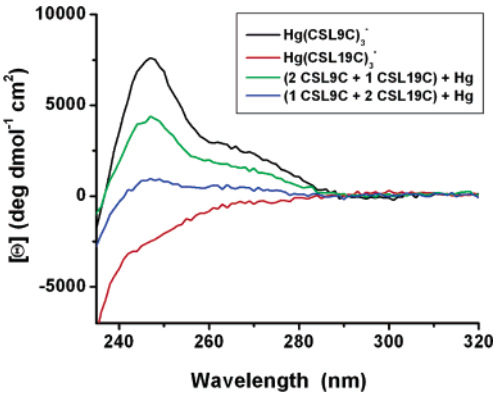

Figure 11. Difference CD spectra of solutions containing 10 μM Hg(II) and different ratios of the peptides CSL9C and CSL19C at pH 9.5 (50 mM CHES buffer).

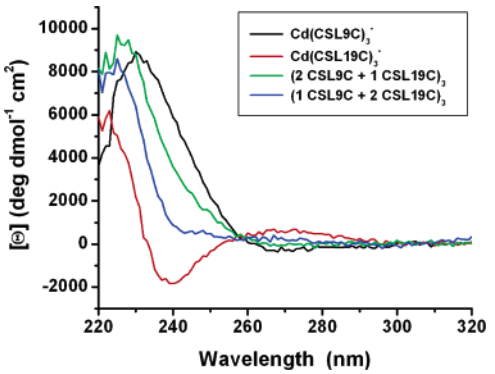

Figure 12. Difference CD spectra of solutions containing 10 μM Cd(II) and different ratios of the peptides CSL9C and CSL19C at pH 8.5 (50 mM TRIS buffer).

CSL9C and CSL19C at pH 9.5. The comparison of the UV−vis spectra observed for the mixtures of peptides with those obtained for the pure $Hg(CSL9C)_3^-$ (black spectrum) and $Hg(CSL19C)_3^-$ (red spectrum) reveals that only two major species are present in solution. The addition of 1 equiv of Hg(II) to a solution containing 2 equiv of CSL9C and 1 equiv of CSL19C generates a spectrum (green line) that closely resembles the spectrum corresponding to a solution that contains two-thirds of the $Hg(CSL9C)_3^-$ species and one-third of the $Hg(CSL19C)_3^-$ species. Consistent with this observation, the addition of 1 equiv of Hg(II) to a solution containing 1 equiv of CSL9C and 2 equiv of CSL19C generates a spectrum (blue line) that, in this case, is similar to the spectrum expected for the presence of one-third of the $Hg(CSL9C)_3^-$ species and two-thirds of the $Hg(CSL19C)_3^-$ species.

(b) CD Spectroscopy. Figure 11 shows the CD spectra corresponding to the addition of Hg(II) to solutions containing different ratios of CSL9C and CSL19C at pH 9.5. The comparison of the transitions observed for the pure homotrimeric Hg(II) complexes, $Hg(CSL9C)_3^-$ (black spectrum) and $Hg(CSL19C)_3^-$ (red spectrum), with those of the mixtures (green and blue spectra) reveals that only two major species are present in solution. The CD spectra of the mixtures correspond to the proportional addition of the respective pure complexes. Figure 12 shows the CD spectra corresponding to the addition of Cd(II) to solutions containing different ratios of CSL9C and CSL19C at pH 8.5. The comparison of the transitions observed for the pure homotrimeric Cd(II) complexes, $Cd(CSL9C)_3^-$ (black spectrum) and $Cd(CSL19C)_3^-$ (red spectrum), with those of the mixtures (green and blue spectra) indicates that only two major species are present in solution. As seen earlier in the case of Hg(II), the CD spectra of the mixtures correspond to the proportional addition of the respective pure complexes. The addition of 1 equiv of Cd(II) to a solution containing 2 equiv of CSL9C and 1 equiv of CSL19C generates a spectrum (green line) that closely resembles the spectrum corresponding to a solution that contains two-thirds of the $Cd(CSL9C)_3^-$ species and one-third of the $Cd(CSL19C)_3^-$ species. In agreement with this observation, the addition of 1 equiv of Cd(II) to a solution containing 1 equiv of CSL9C and 2 equiv of CSL19C generates a spectrum (blue line) that is similar to the spectrum expected for the presence of one-third of the $Cd(CSL9C)_3^-$ species and two-thirds of the $Cd(CSL19C)_3^-$ species.

(c) NMR Spectroscopy. The addition of $^{199}Hg(NO_3)_2$ into solutions containing different ratios of CSL9C and CSL19C at pH 9.6 generates two single peaks appearing at −185 and −313 ppm (parts c and d of Figure 7). These resonances correspond to the formation of the homotrimeric coiled coils $Hg(CSL9C)_3^-$ (Figure 7a) and $Hg(CSL19C)_3^-$ (Figure 7b) and reveal that these two species are the only major species present in solution.

The addition of $^{113}Cd(NO_3)_2$ into a solution containing 2 equiv of TRI L2WL9C and 1 equiv of TRI L2WL23C at pH 8.5 generates two single peaks at 618 and 611 ppm, as shown in Figure 8c. Taking into consideration the ^{113}Cd NMR spectra obtained for the homomeric complexes Cd(TRI L2WL9C)$_3^-$ (Figure 8a) and Cd(TRI L2WL23C)$_3^-$ (Figure 8b), the results obtained here indicate that these two complexes are the major species present in solution under these experimental conditions. Parts c and d of Figure 9 show the ^{113}Cd NMR spectra obtained when $^{113}Cd(NO_3)_2$ was added into solutions containing different ratios of CSL9C and CSL19C at pH 8.5. Two single peaks are observed at 602 and 628 ppm, which correspond to the formation of $Cd(CSL9C)_3^-$ (Figure 9a) and $Cd(CSL19C)_3^-$ (Figure 9b) as major species in solution.

Discussion

Our work has focused on the design of Cys derivatives of the amphipathic TRI family of peptides (TRI LXC). We have shown that these peptides form parallel three-stranded coiled coils above pH 6, generating a thiol-rich binding site that is capable of binding metals such as Hg(II),[4] Cd(II),[44] As(III),[47] Pb(II),[46] and Bi(III).[46] All of these studies have allowed us to gain a deeper understanding of the TRI peptidic system and obtain answers to important issues related to the design of metalloproteins. In particular, we have shown how the aggregation state preferences of these peptides can be exploited to enforce uncommon coordination geometries on a metal, such as Cd(II) and Hg(II), as compared to small molecule thiol ligands in aqueous solutions.[43,44,57,58] Recently, we have improved the design and shown how one can control the coordination number of Cd(II), imposing exclusively a

three- or four-coordination geometry, with minimal sequence changes using nonnatural amino acid.[58] On the other hand, we have also demonstrated how metals can be utilized to control the aggregation state of the coiled coil, enforcing either a lower or a higher aggregation state.[43,44] On the basis of the knowledge that the binding affinity of Cd(II) is dependent on the site of Cys substitution, an **a** site or **d** site, we have also designed a TRI derivative with two binding sites (TRI L9CL19C) that shows sequential and selective binding of Cd(II), first to the **a** site, followed by binding to the **d** site.[59]

One important issue that we have not previously addressed and that we consider crucial for the study of metal insertion and transfer between these metallopeptides is the molecular specifity of the Cys derivatives of these types of coiled coils. First, we were interested in verifying whether our initial design that led to the formation of homotrimeric parallel coiled coils could prevail upon introduction of small changes in the initial sequence. We were specifically interested in modifications that were capable of inducing antiparallel helix aggregation in related systems. Second, we felt it was essential to elucidate how mixtures of the TRI and related peptides that could lead to heteromeric and/or antiparallel coiled coils would behave in the presence of metals. This was especially important when one considers the observations of Ghadiri *et al.*,[24] who demonstrated that single amino acid modifications could convert parallel to antiparallel structures and how the same amino acid sequence could form both parallel and antiparallel aggregations. Thus, while it appeared that our design strategy was successful in solutions containing a single peptide component, there was the possibility that the strength of the resultant metal−S bonds could overcome forces controlling self-assembly of the helices into coiled coils and, consequently, generate less likely aggregating coiled coils in heteromeric mixtures. Taken together with our extensive studies of homomeric coiled coils, studies of heteromeric mixtures allow us to test the overall strength of our peptidic design. The data presented here answered these questions and demonstrated how the TRI LXC family and related coiled coils show molecular specificity in the presence of metals.

We first addressed a single amino acid modification to the TRI peptides because of the hypothesis proposed for the Coil-Ser peptide that the presence of three Trp residues at the same layer was sterically unfavorable, leading to flipping of one of the strands to generate a homotrimeric antiparallel coiled coil.[48] Thus, we generated similar Trp derivatives of the TRI LXC coiled coils. Two peptides, TRI L2WL9C and TRI L2WL23C, were synthesized with the introduction of a Trp residue in the second position of the sequence. Binding of Hg(II) and Cd(II) was studied by UV−vis, and in both cases, the Hg(II) complexes Hg(TRI L2WL9C)$_3^-$ and Hg(TRI L2WL23C)$_3^-$ and the Cd(II) complex Cd(TRI L2WL9C)$_3^-$ were observed, as shown by the growth of the LMCT band at 247 nm for the Hg(II) complexes and at 235 nm for the Cd(II) complex, respectively. These results

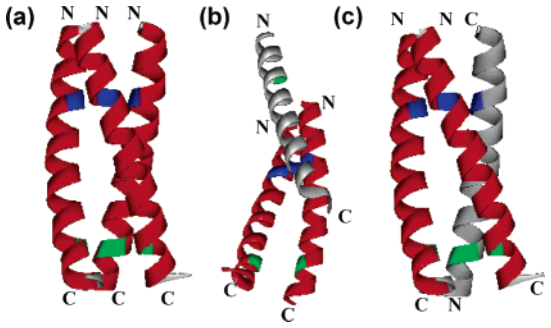

Figure 13. Schematic representations of (a) homotrimeric parallel coiled coil, (b) heterotrimeric parallel coiled coil, and (c) heterotrimeric antiparallel coiled coil. The Cys residue layers are shown in blue and Leu residue layers in green.

indicate the formation of parallel homotrimers because this is the only possible orientation to get a Cys trigonal binding site. Consequently, they suggest that, in the presence of Hg(II) or Cd(II) and at the pH values (8.5−9.6) where the experiments were carried out, our original homomeric parallel design prevails. Recently, we showed that the self-aggregation of the TRI LXC coiled coils drives the formation of the trigonal thiolate Hg(II) and Cd(II) complexes [Hg(TRI LXC)$_3^-$ and Cd(TRI LXC)$_3^-$].[45] On the basis of this study, the effect of introducing Trp into the TRI sequence is a decrease in the self-association affinity of the peptide, which is, consequently, reflected in a weaker affinity of the coiled coils for Hg(II) and Cd(II). However, no effect is observed in the pK_a values for the formation of trigonal Hg(II) and Cd(II) complexes (see Table 2). These observations, taken together, illustrate that the energetic penalty associated with the substitution of Trp for Leu in the second position is solely due to the lowered self-association affinity of the parallel three-stranded coiled coil and is not due to the shifting of the equilibrium from an antiparallel aggregate to the resultant metal-bound, parallel three-stranded form.

To test the nature of association of the peptidic TRI LXC systems more stringently and to begin addressing the issue of molecular specificity, we added first 2 equiv of TRI L2WL9C into the Hg(II) solution, followed by the addition of a third equiv of TRI L2WL23C. Under these conditions and on the basis of the UV−vis spectra, we generated first the linear complex Hg(TRI L2WL9C)$_2$, a result that is consistent with the strong preference of Hg(II) toward thiolates to form a Hg(II)−S_2 bond.[50] The addition of the third equiv of TRI L2WL23C to this linear moiety generated the LMCT band at 247 nm, indicative of the formation of trigonal thiolate Hg(II) complexes. This result ruled out the formation of heterotrimeric parallel coiled coils of the type Hg(TRI L2WL9C)$_{3-n}$(TRI L2WL23C)$_n$ (where $n = 1-2$) because in these cases a Cys trigonal binding site can only be generated if the three helices are slip stacked, hence assembling in such a way as to leave ends of the peptide that were not properly aligned, as shown in Figure 13. Such a configuration is highly energetically unfavorable because it leaves hydrophobic residues exposed to the solvent. The LMCT band obtained for this mixture is very similar to that observed for the formation of the complexes Hg(TRI

(59) Matzapetakis, M.; Pecoraro, V. L. *J. Am. Chem. Soc.* **2005**, *127*, 18229−18233.

L2WL9C)$_3^-$ and Hg(TRI L2WL23C)$_3^-$, suggesting that the mixture of homomeric parallel complexes of two-thirds of Hg(TRI L2WL9C)$_3^-$ and one-third of Hg(TRI L2WL23C)$_3^-$ is formed. An alternative possibility is that the heteromeric antiparallel complex Hg(TRI L2WL9C)$_2$(TRI L2WL23C) results.

To differentiate these possibilities and to characterize the mixture of peptides, we used ^{113}Cd NMR spectroscopy. The ^{113}Cd NMR chemical shifts at 618 and 611 ppm, obtained for peptide samples with 1:3 Cd/TRI L2WL9C and 1:3 Cd/TRI L2WL23C stoichiometries (parts a and b of Figure 8, respectively), are within the range of values that are reported for Cd(SR)$_3^-$ complexes.[60,61] These chemical shifts are consistent with the chemical shifts observed for the Cd(II) complexes seen previously for other members of the TRI LXC family that range from 570−600 ppm, for a pure CdS_3(O/N) form, up to 680−700 ppm, for a pure CdS_3 form. We found that any chemical shift between these values is a reflection of a mixture of CdS_3 and CdS_3(O/N) forms that interconverted rapidly on the NMR time scale generating a single resonance.[44,57,58] The result obtained when Cd(II) was added to a solution containing 2 equiv of TRI L2WL9C and 1 equiv of TRI L2WL23C (Figure 8c) indicates the existence of two distinct species, either because the exchange between them is very slow or because these are two non-interchanging environments for Cd(II). Eluding to earlier results, these resonances correspond precisely to the formation of Cd(TRI L2WL9C)$_3^-$ and Cd(TRI L2WL23C)$_3^-$ in solution. These results clearly and unambiguously indicate that there can be no more than 10% (the detection limits of the experiment) of Cd(II) bound to a heteromeric aggregation of the peptides.

The results using the TRI peptides demonstrated that our initial design was quite robust. However, we felt that it was important to test generally the specificity limits of related three-stranded coiled coils. Thus, we decided to move to the related peptide, Coil-Ser, because the very rationale for introduction of the Trp group in the TRI sequence was based on the pH-dependent strand orientation changes reported for this system. Furthermore, we decided to design one of the peptides with the Cys in a **d** position (19 position) instead of an **a** position (23 position). The rationale behind this new design was based on our extensive studies with the TRI system that showed how substitution of Leu by Cys in an **a** or **d** position generated similar, yet distinctly different, thiol binding sites.[44,46] In particular, we demonstrated by CD how the optical ellipticities of the Hg(II) and Cd(II) complexes of **a** peptides and **d** peptides are opposite, reflecting a different chiral structure around the metal. Consistent with these different environments, distinct ^{113}Cd NMR chemical shifts were observed for the Cd(II) complexes of **a** peptides compared to **d** peptides. The fact that the different locations of the Cys substitution can lead to significant changes in metal binding affinities and spectroscopy allowed us a better handle to evaluate how a mixture of peptides would behave in the presence of metals.

Two derivatives of Coil-Ser were prepared, CSL9C and CSL19C; sequences are provided in Table 1. Position 19 was chosen as the **d** position because if the helix inverts into an antiparallel orientation, Cys19 will be close to the Cys9 generating the trigonal thiol binding site as shown in Figure 13c. Binding of Hg(II) and Cd(II) to either CSL9C or CSL19C was monitored by UV−vis and CD spectroscopies. The UV−vis spectra show the distinctive LMCT band (Figure 5) expected for the formation of the respective trigonal metal complexes Hg(CSL9C)$_3^-$, Hg(CSL19C)$_3^-$, Cd(CSL9C)$_3^-$, and Cd(CSL19C)$_3^-$. The UV−vis titration curves (insets in Figure 5) indicate that, in fact, the stoichiometry of peptide to metal is 3:1 in all cases. As shown in Table 2, the Hg(II) complexes of CSL9C and CSL19C have different UV−vis spectral features with $\lambda_{max} = \sim$247 nm ($\Delta\epsilon \sim 15\,500$ M^{-1} cm^{-1}) and ~229 nm ($\Delta\epsilon \sim 17\,000$ M^{-1} cm^{-1}), respectively. However, the Cd(II) complexes show similar UV−vis features with $\lambda_{max} = \sim$235 nm and $\Delta\epsilon \sim 19\,000$−$21\,000$ M^{-1} cm^{-1} for both peptides. The UV−vis pH titrations (Figure 6a) show that Hg(II) binds to CSL9C (**a** peptide, p$K_a = 7.3$) at a lower pH value than it does to CSL19C (**d** site, p$K_a = 8.6$). As Figure 6b shows, the same trend was obtained for binding of Cd(II) to CSL9C (p$K_{a2} =$ 13.2) and CSL19C (p$K_{a2} = 14.6$). This behavior is consistent with the pH dependence of Hg(II) and Cd(II) binding to the TRI LXC peptides, where we found that both metals require higher pH values to bind to the **d** peptides than to the **a** peptides.[44,46] The determined stability constants (Table 2) show that both metals bind more strongly to CSL9C (**a** site) than to CSL19C (**d** site), results that are also in agreement with those obtained for the TRI LXC family. As expected, on the basis of our studies with the TRI LXC family,[44] the LMCT corresponding to the formation of the complexes Hg(CSL9C)$_3^-$, Hg(CSL19C)$_3^-$, Cd(CSL9C)$_3^-$, and Cd(CSL19C)$_3^-$ could be observed by CD spectroscopy. The CD spectra of these complexes (Figures S2 and S3 in the Supporting Information) show that the Hg(II) and Cd(II) complexes of CSL9C (**a** position) and CSL19C (**d** position) give rise to spectra with opposite ellipticities, revealing a different environment around these metals in the two binding sites.

We further characterized these complexes using ^{199}Hg and ^{113}Cd NMR spectroscopies. Both ^{199}Hg and ^{113}Cd NMR chemical shifts are very sensitive to the coordination number and environment of the respective metals. The ^{199}Hg NMR chemical shift at −185 ppm, obtained for a peptide sample with a 1:3 Hg/CSL9C stoichiometry at pH 8.5 (Figure 7a), is consistent with the chemical shifts observed for the complexes Hg(TRIL16C)$_3^-$ (−179 ppm) [4] and Hg(TRI L9C)$_3^-$ (−185 ppm) reported here in Table 2, supporting the formation of a three-coordinate thiolate Hg(II) complex. In the case of CSL19C, the ^{199}Hg NMR chemical shift is observed at −313 ppm (Figure 7b). This resonance is shifted upfield from the signals observed for CSL9C, TRI L9C, and TRI L16C but far from the chemical shift range of −760 to −990 ppm expected for bis(thiolate) Hg(II) complexes.[50,51] We hypothesize that this change in the chemical shift is due to the different environments that surround Hg(II) in CSL19C

(60) Santos, R. A.; Gruff, E. S.; Koch, S. A.; Harbison, G. S. *J. Am. Chem. Soc.* **1991**, *113*, 469−475.
(61) Summers, M. F. *Coord. Chem. Rev.* **1988**, *86*, 43−134.

(**d** binding site) compared to CSL9C (**a** binding site). It may also reflect a difference in the metal geometry in the two sites, with Hg(II) forming a more symmetric trigonal structure in an **a** site while forming a more T-shaped structure in a **d** site. Similar to what was seen previously for the TRI peptides, the ^{113}Cd NMR chemical shifts at 602 and 628 ppm, obtained for peptide samples with 1:3 Cd/CSL9C and 1:3 Cd/CSL19C stoichiometries (parts a and b of Figure 9, respectively), are also within the range of values that are reported for $Cd(SR)_3^-$ complexes.[60,61] Again, similarly to the TRI LXC family, the ^{113}Cd NMR chemical shifts obtained for $Cd(CSL9C)_3^-$ and $Cd(CSL19C)_3$ are most likely indicative of a mixture of CdS_3 and $CdS_3(O/N)$ coordination environments. All of the UV−vis, CD, and ^{199}Hg and ^{113}Cd NMR data presented here infer the formation of parallel coiled coils because this is the only orientation of the helices that can offer three Cys residues to bind the metal ions. Furthermore, these data show that the **a** and **d** metal binding sites are different, giving rise to singular spectroscopic signals that can be used to identify the species present in solution. Considering these results, we conclude that CSLXC peptides bind Hg(II) and Cd(II) in a manner analogous to that of the TRI peptides. Having established the solution properties of the Hg(II) and Cd(II) complexes of CSL9C and CSL19C by ^{199}Hg and ^{113}Cd NMR, UV−vis, and CD spectroscopies, we decided to study how mixtures of these peptides would behave in the presence of these metals.

On the basis of the different spectroscopic features observed for pure **a** and **d** binding sites, we hypothesized that a Hg(II)-binding site formed by a mixture of **a** and **d** sites will generate unique UV−vis spectroscopic features different from those observed for pure **a** and **d** binding sites. However, the UV−vis spectra obtained when Hg(II) was added to solutions containing different equivalents of the peptides CSL9C and CSL19C at pH 9.5 (Figure 10) do not reflect this situation. The comparison of the UV−vis spectra observed for the mixtures of peptides (green and blue spectra) with those obtained for the pure $Hg(CSL9C)_3^-$ (black spectrum) and $Hg(CSL19C)_3^-$ (red spectrum) suggests that only Hg(II) homotrimeric coiled coils are formed in solution. However, we did not observe clear isosbestic points, and we do not know the signature UV−vis spectra of authentic trigonal thiolate Hg(II) complexes of the type $Hg(CSL9C)^p{}_2(CSL19C)^{a-}$ or $Hg(CSL9C)^p(CSL19C)^a{}_2^-$ (superscripts p and a stand for parallel and antiparallel orientations, respectively). If the spectra of a trigonal Hg(II)-binding site, created by a mixture of Cys in positions **a** and **d**, were additive, we might expect spectra very similar to the ones shown in Figure 10. Hence, we could not rule out the presence of these heterotrimeric species and, therefore, we cannot conclude that Hg(II) homotrimeric coiled coils [$Hg(CSL9C)_3^-$ and $Hg(CSL19C)_3^-$] are the only species in solution.

To gain more insight into the species present in solution, we turned to CD spectroscopy. We exploited the fact that this spectroscopic technique was able to detect the LMCT bands of the complexes $Hg(CSL9C)_3^-$ and $Hg(CSL19C)_3^-$ (Figure S2 in the Supporting Information) and that these absorptions showed opposite ellipticities. We believe that these transitions may be the result of the different orientations of Cys rotamers binding to the metal in this chiral environment. In addition, we have to consider the fact that the Cys in the 9 position is between two **d** layers and the Cys in the 19 position is between two **a** layers. This arrangement of the residues could also reflect the different observed spectroscopic signatures. Thus, we have a direct method to distinguish homotrimeric from heterotrimeric coiled coils because, in the last cases, the trigonal Hg(II)-binding sites will be formed by mixtures of Cys in **d** and **a** positions, giving rise to different chiral environments. Consequently, the CD spectra of solutions containing 1 equiv of Hg(II) [10 μM Hg(II)] and different equivalents of the peptides CSL9C and CSL19C at pH 9.5 should reveal crucial information. The spectra obtained (Figure 11) are consistent with the formation of the homotrimeric complexes $Hg(CSL9C)_3^-$ and $Hg(CSL19C)_3^-$ in solution. The transitions observed correspond to the proportional addition of the CD spectra of the pure homotrimeric complexes and indicate that a new chiral binding site is not generated when CSL9C and CSL19C peptides are mixed in solution in the presence of Hg(II). Therefore, from these experiments, we can rule out the presence of heterotrimeric antiparallel forms and conclude that $Hg(CSL9C)_3^-$ and $Hg(CSL19C)_3^-$ are the only species in solution.

We next tested the behavior of mixtures of CSL9C and CSL19C peptides with Hg(II) under more stringent conditions. As was done for the TRI L2WLXC system, we added first 2 equiv of CSL9C into the Hg(II) solution to form the favorable linear thiolate Hg(II) complex $Hg(CSL9C)_2$. To this solution, we added a third equiv of peptide; however, instead of adding CSL9C, we added CSL19C (we also repeated this experiment in reverse using first 2 equiv of CSL19C, followed by 1 equiv of CSL9C). These conditions should kinetically bias the equilibrium initially toward the mixed peptide aggregate, and if a heteromeric antiparallel metal complex is stable, these are the optimal conditions for detecting its existence. However, it should be noted that separate kinetic analysis of Hg(II) binding and exchange in the TRI systems has shown that interconversion between species is fast. Thus, if the antiparallel species are unstable with respect to the formation of homomeric parallel coiled coils, the latter complexes should be kinetically accessible. At the same time, we have independently established that, under these conditions, metal exchange between metalated and unmetallated peptides for a homomeric coiled coil is fast ($<$250 s).[62] Thus, we expect that conversion from $Hg(CSL9C)_2$ to two-thirds of $Hg(CSL9C)_3^-$ and one-third of $Hg(CSL19C)_3^-$ upon the addition of 1 equiv of CSL19C is also a fast process. For reactions under initial conditions of $Hg(CSL9C)_2$ and $Hg(CSL19C)_2$, the final UV−vis and CD spectra are very similar to those obtained when Hg(II) was added to a solution containing a premixture of peptides. The resulting composition upon the addition of CSL9C to $Hg(CSL19C)_2$ or the addition of CSL19C to $Hg(CSL9C)_2$

(62) Ghosh, D.; Pecoraro, V. L. **2006**, manuscript in preparation.

matched the distribution that is calculated for only $(3 - n)/3$ $Hg(CSL9C)_3^-$ and $n/3$ $Hg(CSL19C)_3^-$ species.

To validate that $Hg(CSL9C)_3^-$ and $Hg(CSL19C)_3^-$ are the only species in solution, we used ^{199}Hg NMR spectroscopy. Given the fact that ^{199}Hg NMR chemical shifts are very sensitive to the Hg(II) coordination environment and on the basis of the different resonances obtained for the homotrimeric parallel complexes $Hg(CSL9C)_3^-$ (−185 ppm) and $Hg(CSL19C)_3^-$ (−312 ppm), we hypothesized that sufficiently different ^{199}Hg NMR chemical shifts could be expected for any of the heterotrimeric antiparallel coiled coils. Therefore, direct detection of Hg(II) complexes of homotrimeric parallel or heterotrimeric antiparallel coiled coils can be undertaken if the metal does not migrate between the sites faster than the NMR time scale. Parts c and d of Figure 7 show that the addition of $^{199}Hg(NO_3)_2$ into solutions containing different ratios of CSL9C and CSL91C at pH 9.6 generates two single peaks appearing at −185 and −313 ppm. These resonances correspond to the formation of the homotrimeric coiled coils $Hg(CSL9C)_3^-$ and $Hg(CSL19C)_3^-$ and clearly indicate the non-existence of Hg(II) bound to a heterotrimeric coiled coil. The existence of two resonances is indicative of the presence of two distinct non-interchanging environments for Hg(II) or a slow metal exchange between $(CSL9C)_3$ and $(CSL19C)_3$ on the NMR time scale. These results support the UV−vis and CD data and suggest that Hg(II) homotrimeric parallel coiled coils [$Hg(CSL9C)_3^-$ and $Hg(CSL19C)_3^-$] are the only species in solution that the limit of detection of ^{199}Hg NMR, CD, and UV−vis spectroscopies allow us to see.

The behavior of different mixtures of CSL9C and CSL19C was also studied in the presence of Cd(II). The UV−vis spectroscopy did not generate spectra differentiable enough to be able to obtain any accurate information (Table 2); therefore, only CD and ^{113}Cd NMR spectroscopies were used. The CD spectra of solutions containing 1 equiv of Cd(II) and different equivalents of CSL9C and CSL19C (Figure 12) are consistent with the formation of the homotrimeric complexes $Cd(CSL9C)_3^-$ and $Cd(CSL19C)_3^-$ in solution. The comparison of the transitions observed for the pure homotrimeric Cd(II) complexes with those of the mixtures reveals that the CD spectra of the mixtures correspond to the proportional addition of the respective pure complexes. To further validate these observations, we used ^{113}Cd NMR spectroscopy. Parts a and b of Figure 9 show that the addition of $^{113}Cd(NO_3)_2$ into solutions containing different ratios of CSL9C and CSL19C at pH 8.5 generates two single peaks appearing at 602 and 628 ppm. These resonances correspond to the formation of $Cd(CSL9C)_3^-$ and $Cd(CSL19C)_3^-$ in solution. As observed previously for the TRI L2WLXC peptides, these results indicate either the presence of two distinct non-interchanging environments for Cd(II) or that metal exchange between $(CSL9C)_3$ and $(CSL19C)_3$ is slow on the NMR time scale. However, as before, the results clearly indicate no generation of Cd(II) bound to a heteromeric aggregation of the peptides.

The data presented here clearly show that, under our experimental conditions and in the presence of Hg(II) and Cd(II), both systems, TRI L2WLXC and CSLXC, form homomeric parallel three-stranded coiled coils. In the case of TRI L2WLXC peptides, the results demonstrate that our intended original parallel peptidic design is highly successful. For the CSLXC peptides, our results are consistent with previous studies where fluorescent derivatives of Coil-Ser have been reported to form parallel trimers in aqueous solution at neutral pH.[63] Overall, these results together imply that the electrostatic interactions between the helices, and not the Trp sterics, could be the critical factor controlling the final orientation of the helices in these types of coiled coils. Consistent with these results, the mixtures of peptides for both TRI LXC and CS peptides formed mostly homotrimeric parallel coiled coils in the presence of Cd(II) and Hg(II). This specificity of the nature of the aggregation (homotrimers vs heterotrimers) and orientation of the helices (parallel vs antiparallel) is remarkable, especially if one considers that the only difference in the sequence of these peptides is the position of the Cys residue (Table 1). The following question arises: What drives this specificity to form homotrimeric parallel coiled coils? There are two limiting possibilities that can explain this observed specificity: either the metals induce this recognition or the sequence of the designed peptides encodes this process.

Table 3. Values of $-\Delta G_{assoc}$ (kcal/mol) from Guanidium Denaturation Experiments[a]

peptide	$-\Delta G_{assoc}$ (kcal/mol)[b]	peptide	$-\Delta G_{assoc}$ (kcal/mol)[b]
TRI	23.5 (7.8)[c]	TRI L2WL9C	17.1 (5.7)
TRI L9C	19.4 (6.5)	TRI L12VL16C	16.5 (5.5)
TRI L16C	19.1 (6.4)	TRI L9AL16C	12.8 (4.3)
TRI L12C	18.4 (6.1)	TRI L12GL16C	12.5 (4.2)

[a] See ref 45. [b] Values with parentheses are for a single monomer. [c] See ref 13.

Two main forces, hydrophobic packing and electrostatic interactions, have been postulated to play a crucial role in determining the overall stability and final three-dimensional structure of the coiled coils. We found that, in our TRI system, the disruption of a Leu layer by Cys substitution destabilizes the coiled coils by ∼4−5 kcal/mol (Table 3), independently of the Leu layer disrupted. As expected, the additional replacements of Leu by either more sterically demanding amino acids (Trp) or smaller nonpolar amino acids (Val, Ala, and Gly) destabilize further the coiled coils in a manner that reflects the poorer hydrophobic packing of the final coiled coil. Any of the heterotrimeric parallel combinations of the two families of coiled coils studied here, $M(\text{peptide LXC})^p{}_{3-n}(\text{peptide LX'C})^p{}_n^-$ (where M = Hg(II) or Cd(II), superscript p = parallel, X = position 9, and X′ = positions 19 or 23), will have two layers where the hydrophobic packing is a mixture of Leu and Cys. This implies the disruption of the hydrophobic packing in two Leu layers, and on the basis of Table 3, an energetic penalty of ∼4−5 kcal/mol could be expected compared to the respective homotrimeric parallel species $M(\text{peptide LXC})^p{}_3^-$ or $M(\text{peptide LX'C})^p{}_3^-$. Consistent with this, the heterotri-

(63) Wendt, H.; Berger, C.; Baici, A.; Thomas, R. M.; Bosshard, H. R. *Biochemistry* **1995**, *34*, 4097−4107.

meric coiled coils were not observed with either Hg(II) or Cd(II) because all of our data indicate the formation of a binding site with three Cys residues. However, any of the heterotrimeric antiparallel combinations, M(peptide LXC)$^{p}_{3-n}$(peptide LX′C)$^{a}_{n}{}^{-}$ (where superscript a = antiparallel), that would generate this type of binding site were not observed. In these cases, the hydrophobic core is formed by layers of Leu and one layer of Cys, implying the disruption of only one Leu layer. It should be noted here that, because of the antiparallel orientation, the hydrophobic packing in all of the layers involves a combination of **a** and **d** sites, either **aad** or **dda**. In addition, these coiled coils will present two mismatched electrostatic interfaces, Glu−Glu and Lys−Lys, that in our case seem to be important structure determination factors because these species were not generated despite presenting a better hydrophobic packing than the parallel heterotrimers. On the basis of these observations, the heterotrimeric antiparallel combinations should be at least on the order of 4−5 kcal/mol less stable. Consistent with this, the stabilization of ∼1.2 kcal/mol gained when a third thiolate binds to a linear bis(thiolate) Hg(II) complex is not enough to overcome these unfavorable interactions. Consequently, the addition of the third helix to the linear complexes [peptide LXC + Hg(II)(peptide LX′C)$_2$ or peptide LX′C + Hg(II)(peptide LXC)$_2$] never generated the respective antiparallel heterotrimers.

These results indicate that, in the presence of Hg(II) and Cd(II), these peptides show molecular specificity and the metal−S bonds are not strong enough to overcome this molecular recognition and stabilize alternative aggregation states. Considering that one of the major challenges in coiled coil design is the achievement of specificity in terms of the oligomeric state, with respect to number (two, three, four, or higher), nature (homomers vs heteromers), and strand orientation (parallel vs antiparallel), the two families studied here, TRI and Coil-Ser, represent highly successful systems. Therefore, it is our belief that the TRI peptides are a perfect scaffold to begin addressing important questions such as metal-transfer processes between proteins. At this point, we cannot completely assert that this molecular specificity is encoded in the sequence of peptides. To be able to understand the behavior of the mixtures of these peptides fully in the absence of metals, it would be necessary to use techniques that will allow us to distinguish the different potential populations of peptides that can exist in solution. Bearing in mind that all of the peptides have the same molecular weight (the only change in sequence is the position of the Cys residue), we decided to label them with different fluorescent dyes and use fluorescence resonance energy-transfer spectroscopy to study the peptide association dynamically. These studies are now underway and promise to provide even more detailed information on recognition processes of these "protein ligands". The information obtained will be crucial for understanding the basis of the profound molecular selectivity of these peptides in the presence of metals.

In summary, we have shown that our design for metal binding peptides successfully achieves homomeric parallel three-stranded coiled coils even with mixtures of peptides that could easily adopt other conformations. This is an important achievement given the statistical number of possible variants that were possible (these include two- or four-stranded coiled coils, heteromeric species, and/or parallel and antiparallel orientations within the different aggregates). Furthermore, we have shown that, at least for Hg(II) and Cd(II) in three-coordinate environments, the metal−S bonds are not strong enough to perturb the desired peptide structure. It should be noted, however, that there is still room for improvement in our design because substoichiometric ratios of peptide to Hg(II) (e.g., ratios of 2:1 or less) lead to linear complexes within two-stranded coiled coils. Ultimately, we hope to obtain a design that will always allow for the formation of three-stranded coiled coils, even at these substoichiometric ratios of peptide to metal.

Experimental Section

Materials. F-moc-protected amino acids and the MBHA rink amide resin were purchased from Novabiochem; *N*-hydroxybenzotriazole and 2-(1*H*-benzotriazol-1-yl)-1,1,3,3-tetramethyluronium hexafluorophosphate were bought from Anaspec Inc.; diisopropylethylamine, acetic anhydride, and pyridine were purchased from Aldrich; piperidine was supplied by Sigma; and *N*-methylpyrrolidinone was obtained from Fisher Scientific.

Peptide Synthesis and Purification. All peptides were synthesized on an Applied Biosystems 433A peptide synthesizer by using standard protocols[64] and purified and characterized as described.[43] The stock solution concentrations were determined by using Ellman's test.[65] A list of the peptides synthesized with their sequences is given in Table 1.

UV−Vis Metal Binding Titrations. Metal binding titrations involving homomeric coiled coils of the peptides with Hg(II) were performed by titrating aliquots of a ∼2 mM stock solution of the peptide into a 2.5-mL solution of 10 μM $HgCl_2$ and 50 mM appropriate buffer: phosphate buffer at pH 8.5 for L9C and L23C peptides and CHES buffer at pH 9.5 for L19C peptides. The development of LMCT bands between 200 and 320 nm was monitored on a Carey 100 Bio UV−vis spectrophotometer. All solutions were purged with Ar before titrations to minimize the chances of oxidation. For each addition of peptide, an equivalent addition was made in the background solution containing only 50 mM buffer so that the difference spectra taken could be attributed only to metal−peptide conformational changes. After each addition of aliquot, the solutions were left to equilibrate for 10 min before the reading was taken. For titrations involving more than one peptide, 2 equiv of one peptide was added to the $HgCl_2$ solutions to generate the HgS_2 moiety. This was followed by the addition of the third equiv of the other peptide in an attempt to generate the heteromeric bundles encapsulating trigonal Hg(II). The choice of buffers for these titrations was maintained similarly to the ones provided above. The addition of the second peptide was continued until there was no change in the growth of the LMCT band. Metal binding titrations of these peptides were also conducted with Cd(II) using a similar method, with the only differences being the equilibration time, which was 15 min, and the use of 50 mM TRIS buffer at pH 8.5 for L9C and L23C peptides and 50 mM CHES buffer at pH 9.5 for the L19C peptide.

(64) Chan, W. C.; White, P. D. *Fmoc Solid-Phase Peptide Synthesis: A Practical Approach*; Oxford University Press: New York, 2000.
(65) Ellman, G. M. *Arch. Biochem. Biophys.* **1959**, *82*, 70.

pH titrations were performed by adding small aliquots of 1 mM to 1 M solutions of potassium hydroxide to unbuffered solutions of 10 μM metal salt and 30 or 50 μM peptide that were bubbled with Ar. The equilibration time for each addition of base was at least 10 min. The change in the pH value was monitored using an Accumet gel-filled pencil-thin Ag/AgCl single-junction electrode with an Orion Research digital pH millivolt meter 611. The solutions were constantly purged with Ar, preventing significant buildup of disulfide-linked peptide dimers. Reverse titrations were performed by adding small aliquots of 1 mM to 1 M solutions of hydrochloric acid, and the pH titration curves obtained were essentially identical.

CD Spectroscopy. All CD spectroscopy experiments were performed on an AVIV 62DS spectrometer using 1-cm strain-free quartz cuvettes. The peptide concentration for each experiment was maintained at 30 μM (in monomer concentration), and the metal concentration was kept at 10 μM. All metal binding titrations were performed in the presence of 50 mM of the appropriate buffer. Spectra were collected at 25 °C from 320 to 230 nm every 1 nm with 1 s for signal averaging.

NMR Spectroscopy. All of the spectra were collected at room temperature on a Varian Inova 500 spectrometer (110.92 MHz for ^{113}Cd and 89.48 MHz for ^{199}Hg) equipped with a 5-mm broadband probe.

(a) ^{113}Cd NMR. ^{113}Cd NMR spectra were externally referenced to a 0.1 M $Cd(ClO_4)_2$ solution in D_2O. A spectral width of 847 ppm (93 897 Hz) was sampled using a 90° pulse (5.0 μs) and a 1-s acquisition time without delay between scans. Samples were prepared by dissolving 20−30 mg of lyophilized and degassed peptide in 450 μL of 15% D_2O under a flow of Ar, followed by the addition of the desired amount of a 250 mM $^{113}Cd(N_3O)_2$ solution (prepared from 95% isotopically enriched ^{113}CdO obtained from Oak Ridge National Laboratory, Oak Ridge, TN) and the adjustment of the pH with KOH or HCl solutions. An Ar atmosphere was maintained when possible, but the samples came in contact with O_2 while the pH was adjusted. The resulting samples contained 9−12 mM peptide, which corresponds to a 3−4 mM three-helix coiled coil. For those experiments where a mixture of peptides was used, stock solutions of the respective peptides in a 15% D_2O solution were prepared and the desired amount of each peptide was used for the particular experiment. The data were processed using the software Mestrec v2.3a. All free induction decays (FIDs) were zero-filled to double the original points and were treated with an exponential function with a line broadening of 50 Hz, unless another way is noted.

(b) ^{199}Hg NMR. ^{199}Hg NMR spectra were externally referenced to 0.1 M $Hg(ClO_4)_2$ in a 0.1 M $HClO_4/D_2O$ solution at −2250 ppm.[48] A spectral width of 1340 ppm (119 940 Hz) was sampled using a 5.0-μs 90° pulse and a 0.05-s acquisition time with a delay between scans of 0.01 s. Samples were prepared as explained above using a stock solution of 125 mM $^{199}Hg(N_3O)_2$ (prepared from 91% isotopically enriched ^{199}HgO obtained from Oak Ridge National Laboratory, Oak Ridge, TN). The data were processed using the same software and procedure as was described for ^{113}Cd NMR. In this case, an exponential function with a line broadening of 100 Hz was used.

Acknowledgment. The authors thank the National Institutes of Health (Grant 5 R01 ES012236-02) for funding the research work conducted.

Supporting Information Available: Listings of models for fitting the UV−vis data, difference UV−vis spectra for TRI L2WL9C binding to Hg(II) and Cd(II), and the CD spectra of the complexes $Hg(CSL9C)_3^-$, $Hg(CSL19C)_3^-$, $Cd(CSL9C)_3^-$, and $Cd(CSL19C)_3^-$. This material is available free of charge via the Internet at http://pubs.acs.org.

IC061183E